ELSEVIER

Nuclear Instruments and Methods in Physics Research A 443 (2000) 331–341

NUCLEAR INSTRUMENTS & METHODS IN PHYSICS RESEARCH
Section A

www.elsevier.nl/locate/nima

Development of new mixed $Lu_x(RE^{3+})_{1-x}$AP:Ce scintillators ($RE^{3+} = Y^{3+}$ or Gd^{3+}): comparison with other Ce-doped or intrinsic scintillating crystals

J. Chval[a], D. Clément[b,c], J. Giba[d], J. Hybler[a], J.-F. Loude[b], J.A. Mares[a,*], E. Mihokova[a], C. Morel[c], K. Nejezchleb[d], M. Nikl[a], A. Vedda[e], H. Zaidi[c]

[a]*Institute of Physics, Academy of Sciences of the Czech Republic, Cukrovarnicka 10, 16253 Prague 6, Czech Republic*
[b]*Institute of High Energy Physics, University of Lausanne, CH-1015 Lausanne, Switzerland*
[c]*Division of Nuclear Medicine, Geneva University Hospitals, CH-1211 Geneva 4, Switzerland*
[d]*Crytur, Palackeho 175, 51119 Turnov, Czech Republic*
[e]*INFM and Dipartimento di Scienza dei Materiali dell'Universita' di Milano, Via Cozzi 53, I-20125 Milano, Italy*

Received 20 May 1999; accepted 22 September 1999

Abstract

This paper presents the development of new Ce-doped, fast and high effective-Z mixed $Lu_x(RE^{3+})_{1-x}$AP:Ce crystals. These crystals have been grown by the Czochralski method and good results have been obtained with $x = 0.1$, 0.2 and 0.3 for Y^{3+} ions and roughly between $x = 0.6$ and 0.7 for Gd^{3+} ions. Relative light yields measured for the $Lu_x(RE^{3+})_{1-x}$AP:Ce crystals are 40–75% higher than for BGO and are comparable to the light yield of YAP:Ce crystal. Measured energy resolutions at 662 keV range over 8–15.3% FWHM and are close to the energy resolution obtained with YAP:Ce. Thermally stimulated luminescence (TSL) measurements above room temperature have also been performed: in accordance with the expected effect of trap states on scintillation efficiency, an anticorrelation between TSL intensity and light yield is found. © 2000 Elsevier Science B.V. All rights reserved.

PACS: 25.20.Dc; 29.40.Mc; 78.55.-m; 78.60.Ya

Keywords: Scintillators; $Lu_x(RE^{3+})_{1-x}$AP:Ce crystals; Light yield; Energy resolution; Luminescence; Thermally stimulated luminescence (TSL)

1. Introduction

At present, $Bi_4Ge_3O_{12}$ (BGO) intrinsic scintillating crystal is the most used one in positron emission tomography (PET) [1]. It is dense ($\rho = 7.13$ g/cm^3), its light yield is about 20–25% of NaI(Tl) [2] with a rather slow scintillation decay constant ($\tau_{sc} \sim 300$ ns) [3]. For the next generation of positron tomographs and coincidence gamma cameras, scintillating crystals should have a high effective-Z (high Z_{eff}) as well as a higher light yield and a faster decay constant than BGO. The most promising materials among new or improved

*Corresponding author. Tel.: + 1-420-2-24311137; fax: + 420-2-3123184.
E-mail address: amares@fzu.Cz (J.A. Mares).

0168-9002/00/$ - see front matter
PII: S0168-9002(99)01066-9

scintillating crystals appear to be Ce-doped crystals such as LSO:Ce, GSO:Ce, as well as Ce-doped orthoaluminate crystals like YAP:Ce and LuAP:Ce [4–15]. YAP:Ce [6], LSO:Ce [5,12] and GSO:Ce crystal of good quality [11] are grown with efficient scintillation properties. On the other hand, growth of large, good quality pure LuAP:Ce crystal has never been reported until now [7–10]. Moreover, a reabsorption process seems to influence its scintillation parameters [7].

At present, LuAP:Ce is a promising scintillation crystal. However, no reliable growth production processes have been demonstrated yet. Today, the Bridgeman method gives better results for growing LuAP:Ce as compared with the Czochralski method. LuAP:Ce samples of $5 \times 5 \times 50$ mm^3 were prepared using the Bridgeman method [8] whereas only very few and small crystal samples could be obtained using the Czochralski method [9,10]. Scintillation properties of LuAP:Ce can vary substantially between different crystals [7,10], and other lutetium phases, especially the garnet phase, can arise in the samples. Growth of LuAP:Ce appears to be extremely delicate since it is very difficult to stabilize the lutetium orthoaluminate phase. A possible way to overcome this problem is to grow mixed orthoaluminate crystals, especially using yttrium or gadolinium [13].

The aim of this study was to develop new, fast and high Z_{eff} Ce^{3+}-doped mixed orthoaluminate $Lu_x(RE^{3+})_{1-x}$AP:Ce crystal scintillators (chemical formula $Lu_x(RE^{3+})_{1-x}AlO_3$:Ce) for $RE^{3+} = Y^{3+}$ or Gd^{3+} ions with higher Ce content (≈ 0.3 at%) than in crystals previously studied [13]. The results of detailed investigations of the crystal composition, absorption, scintillation, luminescence and thermally stimulated luminescence (TSL) are described. These studies were carried out at room temperature and TSL measurements were also obtained at higher temperatures. A comparison with the properties of other Ce^{3+}-doped and intrinsic scintillating crystals is given.

2. Growth and composition of crystals

Orthoaluminate $Lu_x(RE^{3+})_{1-x}$AP:Ce mixed crystals ($RE^{3+} = Y^{3+}$ or Gd^{3+} ions) were grown by the company Crytur (Palackeho 175, Turnov, Czech Republic) using the Czochralski method. The crystals were prepared from almost stoichiometric mixtures of raw and doping materials (oxides of lutetium, yttrium, gadolinium, aluminium and cerium of 3N and 4N purity). These mixtures were heated in a furnace up to 1950°C where liquid phase appeared. By cooling down the mixtures, solidification starts slightly below 1950°C. Melting points of individual crystals have not been measured. Nevertheless, we estimate that the melting points of mixed crystals are around 1880°C and 1950°C, according to the melting points reported in Ref. [4] for YAP:Ce (1875°C) and in Ref. [8] for LuAP:Ce (1960°C). Large crystals (roughly 6 cm long and between 1.5 and 2 cm in diameter) of good quality were grown for Lu_xY_{1-x} AP:Ce with $x = 0.1, 0.2$ and 0.3. These crystals were almost free of extended defects and moreover no garnet phase appeared. Growth of the mixed Lu_xGd_{1-x}AP:Ce crystals was more difficult and acceptable results were obtained for x ranging between 0.6 and 0.7. The reproducibility of crystal

Table 1
Compositions and Ce concentrations of the newly developed mixed Lu_xY_{1-x}AP:Ce and Lu_xGd_{1-x}AP:Ce crystals (accuracy of measurements is $\pm$ 4%)

Crystal	Ce (at%)	Lu (at%)	Y (at%)	Gd (at%)	Al (at%)	O (at%)
$Lu_{0.1}Y_{0.9}$AP:Ce	0.15	2.014	17.86	—	19.99	59.98
$Lu_{0.2}Y_{0.8}$AP:Ce	0.124	2.96	14.08	—	18.13	64.62
$Lu_{0.3}Y_{0.7}$AP:Ce	0.19	5.51	14.24	0.041	20.07	59.98
$Lu_{0.6}Gd_{0.4}$AP:Ce	0.27	10.43	—	8.56	22.39	58.30
$Lu_{0.65}Gd_{0.35}$AP:Ce	0.13	12.82	—	6.37	21.77	59.30
$Lu_{0.7}Gd_{0.3}$AP:Ce	0.17	14.68	—	6.10	22.60	56.58

Table 2
Lattice parameters of $YAlO_3$ (according to Ref. [14]), Lu_xY_{1-x}AP:Ce, Lu_xGd_{1-x}AP:Ce and $LuAlO_3$ crystals (space group is Pbnm). The $LuAlO_3$:Ce crystal was originally described in Ref. [9]

Lattice parameters	*a*	*b*	*c*
$YAlO_3$	5.180(2)	5.330(2)	7.375(2)
$Lu_{0.1}Y_{0.9}$AP:Ce	5.18(2)	5.33(1)	7.36(4)
$Lu_{0.2}Y_{0.8}$AP:Ce	5.17(1)	5.33(1)	7.36(1)
$Lu_{0.3}Y_{0.7}$AP:Ce	5.13(2)	5.33(1)	7.31(5)
$Lu_{0.65}Gd_{0.35}$AP:Ce	5.17(2)	5.33(2)	7.37(3)
$LuAlO_3$:Ce	5.11(2)	5.33(1)	7.33(3)

growth (number of well-grown crystal to total number of growth experiments) for these crystals was about 0.3. Crystals have polycrystalline character with bubbles, precipitates and other mechanical distortions (cracks) and garnet phase arose on their surfaces. Attempts to grow pure LuAP:Ce crystal were unsuccessful and only garnet phase appeared.

The composition and Ce content of mixed orthoaluminate crystals were evaluated by electron beam excited X-ray analysis using JEOL Superprobe JXA733 electron microscope (JEOL Ltd. 1418 Nakagami, Tokyo 196, Japan). Results are presented in Table 1. Generally, $Lu_x(RE^{3+})_{1-x}$ AP:Ce crystals contained between 0.1 and 0.3 at% of Ce. These values are comparable to values usually obtained with well-developed YAP:Ce crystal [6,13,14].

Lattice parameters of some of the mixed $Lu_x(RE^{3+})_{1-x}$AP:Ce orthoaluminate crystals were determined from precession photographs, recorded using Nb-filtered Mo K_α radiation. These parameters for mixed crystals, YAP:Ce [14] and $LuAlO_3$:Ce are presented in Table 2.

3. Measurements

3.1. Sample preparation

Samples for luminescence and scintillation measurements were directly prepared from the Czochralski-grown crystals. Lu_xGd_{1-x}AP:Ce samples were cut out from the most regular parts of the bowles. Some of these crystals were annealed in reducing atmosphere (Ar and a small flow of H_2) at 1200°C for 20 h in order to improve their properties, e.g. to get an increase of Ce^{3+} with respect to Ce^{4+} ions and a decrease of the number of colour centres [16]. Parallelepipeds of $7 \times 7 \times 2$ mm^3 with front and rear faces plus one side face polished were used for luminescence measurements. Special thin samples of $\sim$ 0.3–0.4 mm thickness with polished front and rear faces were prepared for absorption spectra measurements. For scintillation measurements, 10 mm long cylinders with 8 mm diameter with polished faces were used. For comparison, BGO and two other well-developed Ce-doped crystals (YAP:Ce and GSO:Ce) were also measured. For TSL measurements, plates of $10 \times 10 \times 1$ mm^3 were cut and polished.

3.2. Absorption and luminescence measurements

Absorption spectra were measured from 190 to 400 nm using a Shimadzu UV-3101 PC absorption spectrophotometer (Shimadzu Corp., 3, Kanda-Nishikicho 1-chome, Tokyo 101, Japan). Luminescence measurements (emission and excitation spectra and decay kinetics) were carried out in the visible and near-UV range from 200 to 700 nm using a UV and visible spectrofluorometer Edinburgh Instruments 199S (Edinburgh Instruments Ltd., Riccarton, Currie, Edinburgh EH144AP, UK) [13]. Luminescence decay curves were measured in the time range up to a few μs with a time resolution of about 0.6 ns using the single photon counting method. Scintillation decay curves were observed under 511 keV photon excitation using a ^{22}Na radioactive source.

3.3. Measurements of energy resolutions and relative light yields

Measurements of energy resolutions and relative light yields were carried out using a ^{137}Cs radioactive source. Crystals were wrapped in 5–6 layers of Teflon™ and were directly coupled to the photocathode of a Philips 2020Q photomultiplier (PMT) using a silicon oil. The ^{137}Cs source was not collimated and was placed about 1 cm away from the entrance face of the crystal.

A discriminator threshold set on the PMT pulse height was used to trigger events by gating simultaneously one LRS 2249sg and three LRS 2249W charge ADCs. Time gates were adjusted to integrate the collected charge over 100, 200, 500, 1000 and 2000 ns. The LRS 2249 sg was gated using 100 and 200 ns strobe signals, and the three LRS 2249W were gated using 500 ns, 1 and 2 μs signals, respectively. With the long gate durations (1 or 2 μs), the so-called "prompt" light yield was measured [15]. All measured crystals have a principal scintillation decay constant lower than 300 ns with eventual small contributions from other slow components. With shorter time gates (between 100 and 500 ns), the so-called "fast" light yield of crystals was measured. Due to their fast scintillation decay constants (about 30 ns) [4,6,16,17], the prompt and fast light yields are similar for YAP:Ce and Lu_xY_{1-x}AP:Ce.

Pulse tail signals shorter than 100 ns with increasing amplitudes were used to determine the gains of the five ADC channels. ADC gains after subtraction of the pedestals were then used to normalize the pulse height spectra to the energy spectrum obtained with a 2 μs charge integration time gate.

3.4. *Thermally stimulated luminescence (TSL) measurements*

TSL measurements were carried out after X-ray irradiation using a Machlett OEG 50 (tungsten target) X-ray tube operated at 30 kV from room temperature (RT) up to 300°C with a linear heating rate of 1°C/s. The TSL signal was detected in photon counting mode by using an EMI 9635 QB photomultiplier. Wavelength-resolved measurements were also performed by a home-made TSL spectrometer featuring a double stage microchannel plate followed by a diode array.

4. Results

4.1. *Absorption spectra*

Absorption spectra of $Lu_{0.3}Y_{0.7}$AP:Ce and $Lu_{0.65}Gd_{0.35}$AP:Ce crystals are presented in Fig. 1.

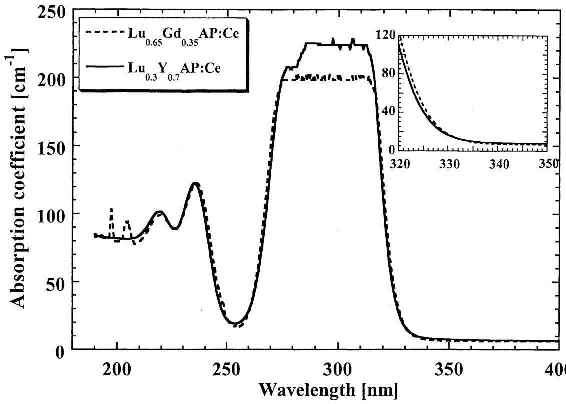

Fig. 1. Absorption spectra of the $Lu_{0.3}Y_{0.7}$AP:Ce and $Lu_{0.65}Gd_{0.35}$AP:Ce crystals measured at RT (sample thickness was 0.35 and 0.39 mm, respectively). In the right top (inset) the long-wavelength tail of the main Ce^{3+} absorption band is displayed.

No significant differences were observed by varying the composition of the crystals. These spectra consist of broad Ce^{3+} bands peaking at about 219 and 235 nm followed by a very strong absorption extending from 260 to 320 nm ($4f^1 \rightarrow 5d^0$ transitions); moreover, Lu_xGd_{1-x}AP:Ce crystals also display narrow Gd^{3+} lines within the range 195–210 nm. To avoid saturation in the absorption measurements due to strong Ce^{3+}-related absorption bands, sample thickness below 0.1 mm would be necessary, but the preparation of such samples is difficult and it was unsuccessful. For the $Lu_{0.3}Y_{0.7}$AP:Ce crystal, intrinsic Ce^{3+} absorption coefficient ranges from 0.1 to 5 cm^{-1} in the long wavelength tail of the main Ce^{3+} absorption band in the range 350 to $\sim$ 330 nm (see inset of Fig. 1). Background absorption due to scattering in the samples is around $\sim 7\ cm^{-1}$. Emission and excitation spectra overlap in this region, especially for the YAP:Ce and Lu_xY_{1-x}AP:Ce crystals (see Figs. 2 and 3). Besides broad Ce^{3+} absorption bands and narrow absorption Gd^{3+} lines, other absorption bands are probably present below 250 nm. These bands are probably connected with some unknown impurities, intrinsic centres and the enhanced light scattering at the sample surfaces cannot be excluded, even if the amplitude of the latter effect does not essentially contribute even at the shortest wavelengths around 200 nm.

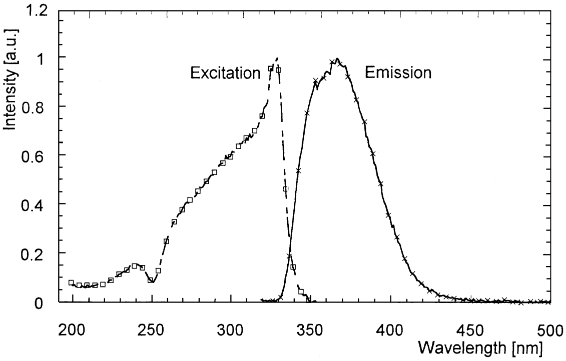

Fig. 2. Emission and excitation spectra of the $Lu_{0.3}Y_{0.7}$AP:Ce crystal measured at RT under excitation $\lambda_{ex} = 300$ nm (emission spectrum) and at $\lambda_{em} = 360$ nm (excitation spectrum).

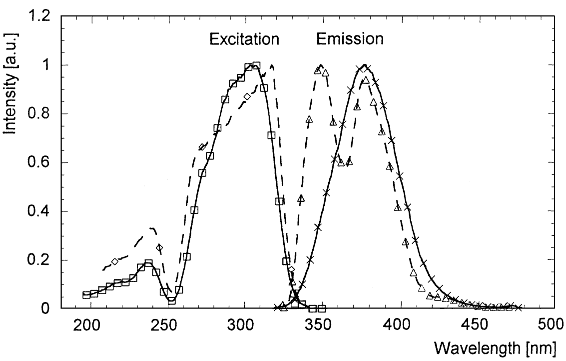

Fig. 3. Emission and excitation spectra of the $Lu_{0.1}Y_{0.9}$AP:Ce crystal measured at RT in the edge of the crystal (solid lines) and in the centre of the crystal (dashed lines). Emission spectra were excited by $\lambda_{ex} = 300$ nm and excitation spectra were measured at $\lambda_{em} = 375$ nm.

4.2. Luminescence spectra and decays

For both Lu_xY_{1-x}AP:Ce and Lu_xGd_{1-x}AP:Ce, luminescence measurements showed almost the Ce^{3+} emission band, with only small variations of the excitation spectra (see Fig. 2 and Ref. [18]). This was valid only for good-quality samples cut from well-grown parts of the crystals. Larger differences between Ce^{3+} emission and excitation spectra appeared when crystal parts with a higher concentration of extended defects were also considered. Fig. 3 presents the spectra measured on different parts of the $Lu_{0.1}Y_{0.9}$AP:Ce sample along its diameter. New Ce^{3+} emission band peaking at $\lambda_p \sim 350$ nm (see Fig. 3) is probably due to other Ce^{3+} ion positions in the crystal. The non-equivalent positions in crystals arise probably close to the defects presented in these parts of crystals (different distribution of Ce^{3+} ions, defects such as grain boundaries, facets, precipitates, etc.). Around these defects Ce^{3+} non-equivalent centres can be affected by the changed local crystal field, which may result in different positions and splitting of Ce^{3+} 5d energy levels.

The observed broad emission and excitation bands are due to the Ce^{3+} $5d^1 \rightarrow 4f^0$ and $4f^1 \rightarrow 5d^0$ allowed electric dipole–dipole transitions, respectively. Luminescence decays of every crystal are characterized by the presence of a fast decay component with $\tau_f \approx 15$–20 ns. However, decays of the Lu_xGd_{1-x}AP:Ce crystals also displayed significant contribution of the slow components ($\tau_{sl} \approx 70$–150 ns). It was observed that the contribution of these slow components decreases by increasing the Ce content [18–20]. Moreover, every crystal including YAP:Ce showed other much slow decay components with decay constants ranging from 1 to 4 μs [4,19,20]. The intensities of slow decay components are higher for the Lu_xGd_{1-x}AP:Ce crystals than for the other crystals [18].

4.3. Energy resolutions and relative light yields

Gamma-ray spectra of a ^{137}Cs source obtained with the $Lu_x(RE^{3+})_{1-x}$AP:Ce crystals using this source were measured to determine their energy resolutions and light yield relative to BGO. The 662 keV total energy peak was fitted by a Gaussian curve plus a linear background using the function

$$f(x) = P_1 e^{-(1/2)((x-P_2)/P_3)^2} + P_4 + xP_5 \quad (1)$$

where P_1, P_2, P_3, P_4, and P_5 are the parameters of the fit. Energy spectra measured using a 500 ns charge integration time gate are shown in Figs. 4, 5 and 7 for YAP:Ce, $Lu_{0.3}Y_{0.7}$AP:Ce and $Lu_{0.65}Gd_{0.35}$AP:Ce crystals, respectively. Fig. 6 shows the spectra obtained for the $Lu_{0.3}Y_{0.7}$AP:Ce crystal using a 2 μs charge integration time gate. The parameters of the fits, their

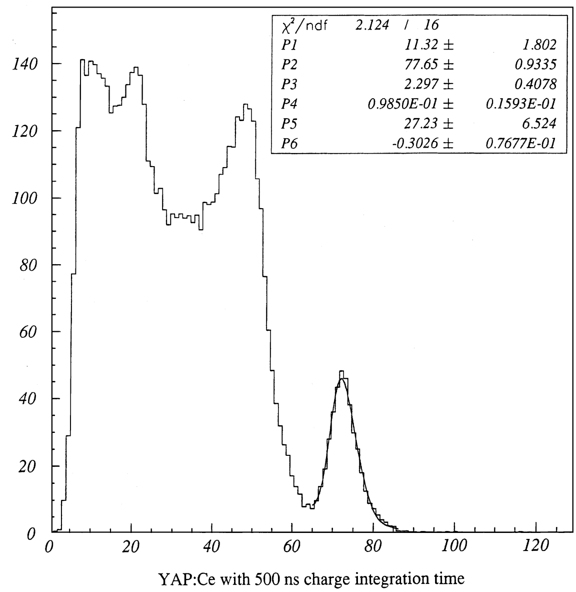

Fig. 4. Gamma-ray spectrum of a ^{137}Cs source measured with the YAP:Ce crystal using a charge integration duration of 500 ns (inset – fitting parameters and errors).

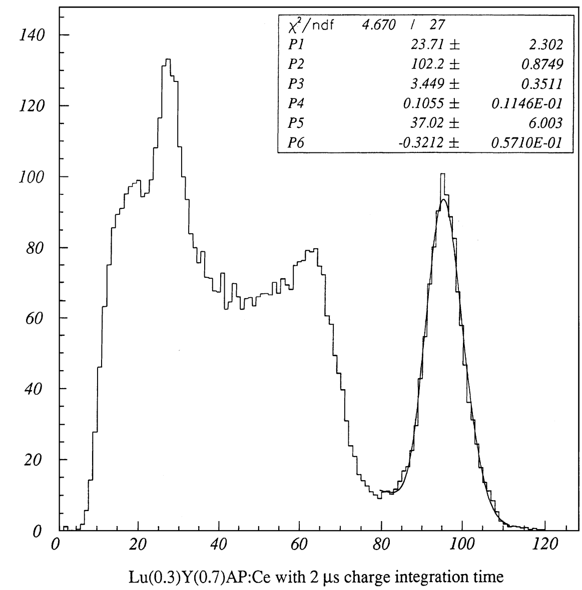

Fig. 6. Gamma-ray spectrum of a ^{137}Cs source measured with the $Lu_{0.3}Y_{0.7}AP$:Ce crystal using a charge integration duration of 2 μs (inset – fitting parameters and errors).

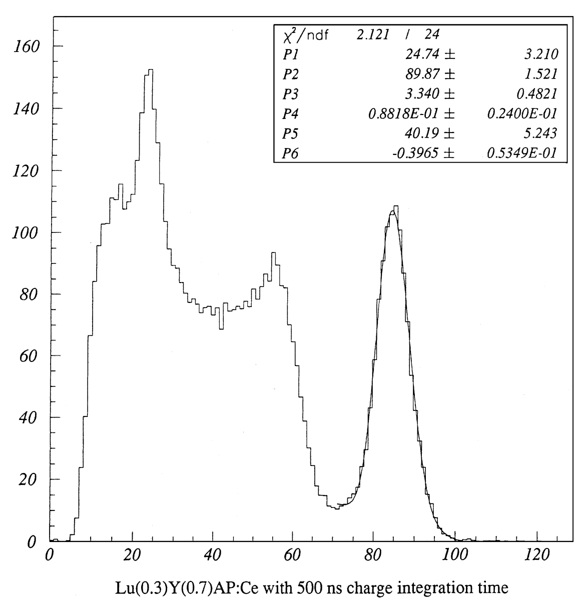

Fig. 5. Gamma-ray spectrum of a ^{137}Cs source measured with the $Lu_{0.3}Y_{0.7}AP$:Ce crystal using a charge integration duration of 500 ns (inset – fitting parameters and errors).

errors, as well as the Chi-square values of the fits are given together with the spectra. Fairly good fits according to Eq. (1) were obtained for the $Lu_{0.65}Gd_{0.35}AP$:Ce crystal, for the BGO and GSO:Ce crystals, but not for the YAP:Ce and mixed $Lu_xY_{1-x}AP$:Ce crystals. This may be due to non-negligible self-absorption processes, probably in the near-UV range around 310–340 nm where Ce^{3+} absorption (excitation) and emission spectra overlap.

Following this hypothesis, we used a simple model to include a linear optical self-absorption coefficient μ_{sa} in the fit of the spectra obtained for orthorhombic crystals containing Y^{3+} ions. The number of detected gamma photons N_γ was parametrized as a function of the depth-of-interaction y along the crystal:

$$N_\gamma(y) \propto \frac{e^{-\mu_{tot} y}}{(D - L + y)} = R_\gamma \tag{2}$$

where y, D, L, μ_{tot} are the distance from the entrance face of the crystal, the distance between the ^{137}Cs source and the photocathode of the PMT, the length of the crystal, and the total linear attenuation coefficient for 662 keV gamma rays, respectively. The number of scintillation photons $N_{h\nu}$ arriving at the photocathode is then proportional to

$$N_{h\nu} \propto e^{-\mu_{sa}(L-y)}. \quad (3)$$

Under these assumptions, the fits of the spectra were obtained using the sum of the contributions of the detected gamma rays within equally spaced transaxial slices of the crystal cylinders. For each slice lying at a depth y from the entrance face of the crystal, the contribution of the detected gamma rays was parametrized using the following equation:

$$f_y(x) = P_1 R_\gamma e^{-(1/2)((x-P_2 R_{h\nu})/P_3\sqrt{R_{h\nu}})} + P_5 + xP_6 \quad (4)$$

with

$$R_{h\nu} = e^{-P_4(L-y)} \quad (5)$$

where P_4 is the parameter which estimates μ_{sa} in cm^{-1}. For each crystal, μ_{tot} was calculated at 662 keV using the GEANT parametrizations of photon cross-sections [21].

This model gave acceptable fits for orthorhombic crystals containing Y^{3+} ions (Figs. 4–7). Significant variations of 10–15% compared to the fit given by Eq. (1) occurred for the parameter P_2 which reflects the intrinsic light yield of the crystal. The linear optical self-absorption coefficient for the YAP:Ce and Lu_xY_{1-x}AP:Ce crystals varied between 0.1 and 0.15 cm^{-1} with a statistical accuracy of about 15% and was reproducible using different charge integration time gates for a given crystal. From Fig. 1 the evaluated intrinsic Ce^{3+} absorption coefficient of the mixed $Lu_{0.3}Y_{0.7}$AP:Ce crystal is between 5 and 0.1 cm^{-1} in the spectral range 330–350 nm.

However, these values hold for monochromatic radiation. Considering that the overlap of Ce^{3+} emission and excitation bands represents roughly 5% of their total widths, the effective linear self-absorption coefficient should be around 0.25–0.005 cm^{-1}. It is in fair agreement with the estimated values of the linear self-absorption coefficients for YAP:Ce and Lu_xY_{1-x}AP:Ce crystals using the above-described fitting procedure.

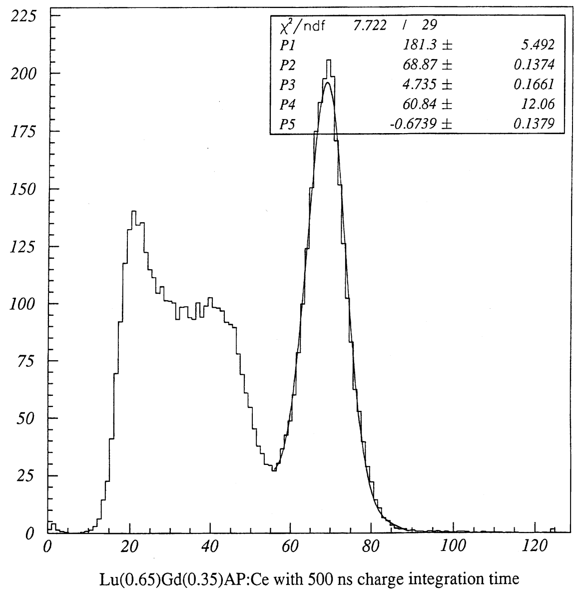

Fig. 7. Gamma-ray spectrum of a ^{137}Cs source measured with the $Lu_{0.65}Gd_{0.35}$AP:Ce crystal using a charge integration duration of 500 ns (inset – fitting parameters and errors).

Light yields were determined relative to the light yield of BGO crystal. A correction factor taking into account the quantum efficiency of the photocathode was calculated over the whole range of the emission spectrum of each crystal. As a result of these calculations, assuming that the charges were entirely collected using a charge integration time gate of 2 μs, the $Lu_{0.3}Y_{0.7}$AP:Ce crystal produces about 1.8 times more light than BGO with more than 80% of its emission response contained within the first 200 ns. Results of energy resolution and relative light yield measurements are summarized in Table 3.

Among all measured Lu_xY_{1-x}AP:Ce crystals, the best one was $Lu_{0.3}Y_{0.7}$AP:Ce whose light yield exceeded that of the YAP:Ce crystal. However, its energy resolution was not better than 8% FWHM compared to 6.8% FWHM obtained for YAP:Ce (see Table 3). This difference might be either due to more self-absorption of the scintillation light which was not taken into account by our crude fitting model or, more probably, to some unknown non-linear emission processes occurring in the crystal. Indeed, light yield and energy

Table 3
FWHM energy resolutions ($\Delta E/E$) for 2 μs and 100 ns charge integration durations and relative light yields of measured crystals to BGO determined using a charge integration duration of 2 μs. Ratios between light yields estimated using respectively 100, 200, 500 and 1000 ns charge integration durations and 2 μs (x ns/2 μs) are also given

Crystal	$\Delta E/E$ (2 μs)	$\Delta E/E$ (100 ns)	Relative light yield (2 μs gate)	100 ns/2 μs	200 ns/2 μs	500 ns/2 μs	1000 ns/2 μs
BGO	16.0%	33.0%	100	21.4%	41.5%	77.4%	94.4%
GSO:Ce	11.5%	13.9%	121	60.0%	87.2%	96.0%	98.3%
YAP:Ce	6.8%	6.4%	136	89.9%	99.5%	98.9%	99.5%
$Lu_{0.1}Y_{0.9}$AP:Ce	8.5%	8.7%	147	70.4%	81.8%	90.6%	96.7%
$Lu_{0.2}Y_{0.8}$AP:Ce	9.9%	9.7%	119	65.4%	78.3%	88.4%	98.9%
$Lu_{0.3}Y_{0.7}$AP:Ce	8.0%	9.2%	178	66.1%	79.9%	87.9%	95.6%
$Lu_{0.65}Gd_{0.35}$AP:Ce	15.3%	19.3%	137	48.2%	69.4%	86.4%	94.4%

resolutions presented in this paper are independent of self-attenuation and therefore represent intrinsic characteristics of the measured crystals near the scintillation emission point rather than effective characteristics at the exit of the crystal with regard to self-absorption. Considering the $Lu_{0.65}Gd_{0.35}$AP:Ce crystals, their energy resolution was more than twice the energy resolution measured in YAP:Ce, but with an equivalent light yield and no noticeable self-absorption. This implies that, as for LSO:Ce where energy resolution appears to be lower than what would theoretically allow its light yield, there are some unknown non-linear processes occurring in the $Lu_{0.65}Gd_{0.35}$AP:Ce crystal which degrades significantly its energy resolution.

4.4. Thermally stimulated luminescence

Glow curves of the Lu_xY_{1-x}AP:Ce, YAP:Ce and Lu_xGd_{1-x}AP:Ce crystals in the temperature range RT–300°C are reported in Figs. 8 and 9, respectively. In the first case, several glow peaks are detected and their intensities are strongly dependent upon the composition of the crystals; on the other hand, Lu_xGd_{1-x}AP:Ce crystals display quite broad and unresolved TSL structures. These measurements were obtained with an X-ray dose of approximately 1 Gy (value evaluated in air). The behaviour of the TSL signal upon X-ray dose was checked for the $Lu_{0.2}Y_{0.8}$AP:Ce and $Lu_{0.65}Gd_{0.35}$AP:Ce crystals: a linear dependence

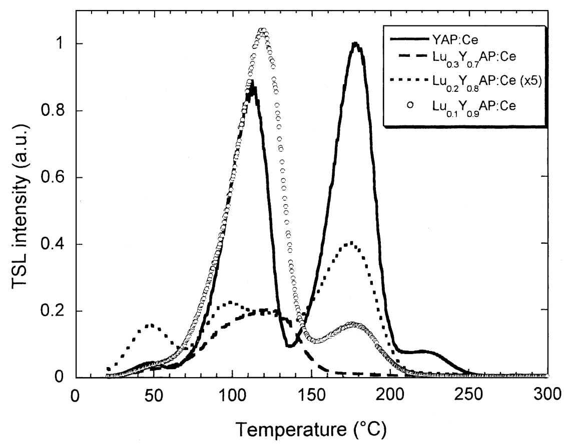

Fig. 8. TSL glow curves of Lu_xY_{1-x}AP:Ce samples obtained after X-ray irradiation at RT.

was found in the range from 0.01 to 1 Gy. The TSL emission spectra display only one band centred at 360 nm, which can be ascribed to the Ce^{3+} emission in agreement with the emission spectra.

Table 4 compares scintillation light yields of the crystals with the values of the TSL signal integrated from 20°C to 300°C (TSL data are normalized with respect to YAP:Ce data). Two other important characteristics of the crystals such as their density ρ and effective-Z (Z_{eff}) are also included in this table. Z_{eff} characterizes the "effective atomic number" of the crystal or its X-ray or γ-ray absorption ability. For compounds consisting of three or four elements as the measured crystals Z_{eff} can be evaluated according to a type of interaction mechanism from atomic masses and numbers of the individual elements and their content in the compounds [22]. Linear attenuation coefficients for 662 keV γ photons calculated using the GEANT parametrizations of photon cross-sections for $Lu_x(RE^{3+})_{1-x}$AP:Ce and YAP:Ce crystals are summarized in Table 5.

5. Discussion and conclusion

Mixed $Lu_x(RE^{3+})_{1-x}$AP:Ce orthoaluminate crystals represent a transition step from the well-known fast but less dense YAP:Ce crystal to the fast and very dense, pure LuAP:Ce crystal. The latter is presently still under development. The mixing of Lu with Y^{3+} or Gd^{3+} ions has led to a better stabilization of the Czochralski-grown orthoaluminate phases as compared to the growth of pure LuAP:Ce.

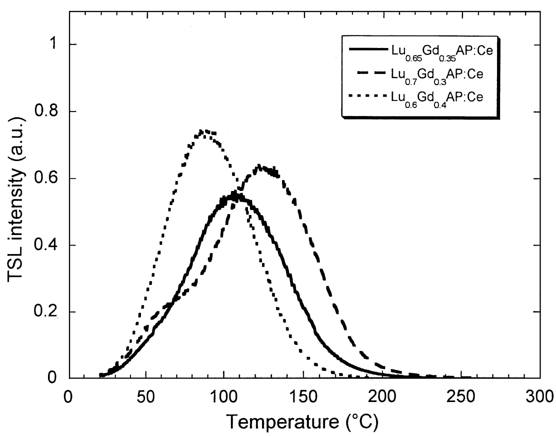

Fig. 9. TSL glow curves of Lu_xGd_{1-x}AP:Ce samples obtained after X-ray irradiation at RT.

The study of mixed $Lu_x(RE^{3+})_{1-x}$AP:Ce orthoaluminate crystals confirmed that: (i) their density is higher than that of YAP:Ce, especially in the case of Lu_xGd_{1-x}AP:Ce crystals, (ii) Ce concentration is in the range of about 0.2 at% up to 0.3 at% and is comparable to that obtained in YAP:Ce or GSO:Ce, (iii) light yields exceed that of BGO by more than 40%, and in some cases more than 75%, and are equal or even higher with respect to YAP:Ce and GSO:Ce, and (iv) energy resolution at 662 keV ranges from 8.0% to 15.3% FWHM and this is comparable to that of YAP:Ce and GSO:Ce. Unlike YAP:Ce for which the intensity of a slow component reaches only 3–6% of its fast component [19], mixed orthoaluminate crystals displayed comparable contribution of the fast ($\tau_f \approx 15$–30 ns) and slow decay components ($\tau_{slow} \geqslant 100$ ns or even more, especially in the case of Lu_xGd_{1-x}AP:Ce crystals). Further investigation would be needed to understand the nature of these slow scintillation decay components.

A number of investigations on TSL properties of scintillating Ce-doped crystals have been recently published [15,17,23,24]. The ratio between "TSL light yield" (defined as the number of photons

Table 4
Relative light yields of crystals to BGO, their TSL signals integrated over 20–300°C (evaluated dose of X-ray in air: 1 Gy) normalized to YAP:Ce results, densities and effective-Z (Z_{eff}) values presented for YAP:Ce and the newly developed Lu_xY_{1-x}AP:Ce and Lu_xGd_{1-x}AP:Ce crystals

Crystal	Relative light yield (BGO – 100)	Relative TSL (YAP:Ce – 1)	ρ (g/cm^3)	Z_{eff} [a]
YAP:Ce	136	1	5.36	34
$Lu_{0.1}Y_{0.9}$AP:Ce	147	0.7	5.73	43
$Lu_{0.2}Y_{0.8}$AP:Ce	119	0.1	5.92	49
$Lu_{0.3}Y_{0.7}$AP:Ce	178	0.2	6.19	53
$Lu_{0.6}Gd_{0.4}$AP:Ce	—	0.8	7.84	62
$Lu_{0.65}Gd_{0.35}$AP:Ce	137	0.6	7.93	63
$Lu_{0.7}Gd_{0.3}$AP:Ce	—	~ 0.8	8.0	63

[a] Appr. – see Ref. [23].

Table 5
Linear attenuation coefficients for 662 keV photons interacting in YAP:Ce and in the newly developed $Lu_xY_{1-x}AP$:Ce and $Lu_xGd_{1-x}AP$:Ce crystals calculated using the GEANT parametrizations of photon cross-sections

Crystal	Total (cm^{-1})	Photoelectric (cm^{-1})	Compton (cm^{-1})	Rayleigh (cm^{-1})
YAP:Ce	0.40	0.01	0.39	0.006
$Lu_{0.1}Y_{0.9}AP$:Ce	0.44	0.03	0.41	0.009
$Lu_{0.2}Y_{0.8}AP$:Ce	0.47	0.04	0.42	0.011
$Lu_{0.3}Y_{0.7}AP$:Ce	0.51	0.06	0.43	0.015
$Lu_{0.6}Gd_{0.4}AP$:Ce	0.66	0.13	0.51	0.026
$Lu_{0.65}Gd_{0.35}AP$:Ce	0.66	0.13	0.51	0.027
$Lu_{0.7}Gd_{0.3}AP$:Ce	0.67	0.13	0.51	0.027

emitted during heating per unit absorbed dose) and prompt scintillation light yield appeared to be the lowest for YAP:Ce ($\sim$ 0.02) while it was around 0.1 for the heavier LuAP:Ce and LSO:Ce [15,24]. Depending on their thermal depth, the trap levels responsible for TSL glow peaks can seriously affect the shape of the scintillation decay or the light yield of a material. Actually, it was found that in YAP:Ce, the electrons released from shallow traps observable at low temperatures contribute significantly to the Ce scintillation (roughly from 25% up to 42%), and simultaneously they are responsible for slowing down of the decay [17]. Glow peaks observed at high temperatures are related to traps characterized by long decay times at room temperature (from several minutes, up to days and even years for the most stable ones), so that one can exclude the effect of these trap levels on the shape of scintillation decay. However, trapping of electrons at such "deep" states during irradiation represents a competitive process with respect to prompt scintillation [15] and can decrease the light yield of the material. This problem may in principle be overcome by reaching a complete trap filling (trap saturation). Nevertheless, such condition is difficult to obtain in practice, due to the very high doses needed in several cases and due to the possible occurrence of continuous detrapping of carriers from less stable traps at room temperature.

The results displayed in Figs. 8 and 9 show that trap levels are strongly influenced by crystal composition: in fact, large variations of the glow curve shape are observed in both the $Lu_xY_{1-x}AP$:Ce and the $Lu_xGd_{1-x}AP$:Ce sample series. Table 4 reports the TSL signals integrated from 20°C up to 300°C and normalized to YAP:Ce data. Similar values were obtained for the $Lu_xGd_{1-x}AP$:Ce crystals, while larger differences can be noticed for $Lu_xY_{1-x}AP$:Ce. In any case, all the $Lu_x(RE^{3+})_{1-x}AP$:Ce crystals show lower TSL signals with respect to YAP:Ce. It is interesting to compare the light yield data of the $Lu_xY_{1-x}AP$:Ce crystals, also reported in Table 4, with their relative TSL signals. Expect the $Lu_{0.2}Y_{0.8}AP$:Ce sample, an opposite correlation between light yield and TSL values was observed, in accordance with the expected effect of such trap states on the scintillation efficiency. It is not straightforward to explain the anomalous behaviour of the $Lu_{0.2}Y_{0.8}AP$:Ce crystal. In this case, very low values of light yield and TSL are observed: non-radiative recombination paths occurring during both the scintillation and the TSL process could possibly account for the observed results. This crystal differed from the others in the sense that it contained an excess of oxygen (see Table 1): this could affect the character and concentration of point defects and could give rise to different light yield and TSL characteristics. More details about the influence of traps – especially shallow ones – on light yield as well as on Ce^{3+} fast and slow decay components can be obtained from low-temperature TSL glow curves (below RT). These low-temperature TSL measurements, together with investigations of transfer processes between Gd^{3+} and Ce^{3+} ions in mixed crystals are currently being carried on.

Among the crystals that we studied, the $Lu_{0.3}Y_{0.7}$AP:Ce crystal seems to be the most promising as for the light yield, energy resolution and scintillation decay constant. Moreover, its TSL intensity is low as well. The effect of self-absorption that was presumably observed needs to be evaluated more carefully. Nevertheless, for medical application such as PET (where the stopping power of the detector is rather important) Lu_xY_{1-x}AP:Ce compounds with $x \leqslant 30\%$ cannot really compete with LSO:Ce or possibly even with pure LuAP:Ce [5,10,12,23,24]. Lu_xGd_{1-x}AP:Ce crystals with $x \geqslant 60\%$ seem to be more interesting in this perspective. To improve the stopping power of the mixed orthoaluminate crystals it requires to increase significantly their lutetium content. With respect to this fact it is necessary to put more effort in growing *almost* pure LuAP:Ce crystal where the content of Y^{3+} or Gd^{3+} ions should be kept at the lowest possible concentrations in order to stabilize the perovskite phase of the crystal during the growth.

Acknowledgements

The authors are grateful to the members of the CERN Crystal Clear Collaboration, and especially Stefaan Tavernier for fruitful discussions. This work was supported by the Institutional Partnership research programme of the Swiss National Science Foundation, grant7 IP 051218, and partly by the grant 203/99/0067 of the Grant Agency of the Czech Republic.

References

[1] K. Wienhard, Phys. Med. XII, (suppl. 1) (1996) 28.
[2] E. Sakai, IEEE Trans. Nucl. Sci. NS- 34 (1987) 418.
[3] C.L. Melcher, J.S. Schweitzer, A. Liberman, J. Simonetti, IEEE Trans. Nucl. Sci. NS-32 (1985) 529.
[4] S. Baccaro, K. Blazek, F. de Notaristefani, P. Maly, J.A. Mares, R. Pani, R. Pellegrini, A. Soluri, Nucl. Instr. and Meth. A 361 (1995) 209.
[5] M. Moszynski, M. Kapusta, D. Wolski, M. Szawlowski, W. Klamra, IEEE Trans. Nucl. Sci. NS-44 (1997) 436.
[6] M. Moszynski, W. Kapusta, D. Wolski, W. Klamra, B. Cederwal, Nucl. Instr. and Meth. A 40 (1998) 157.
[7] C. Dujardin, C. Pedrini, W. Blanc, J.C. Gacon, J.C. van't Spijker, O.W.V. Frijns, C.W.E. van Eijk, P. Dorenbos, A. Fremunt, F. Tallouf, S. Tavernier, P. Bruyndonckx, A.G. Petrosyan, IEEE Trans. Nucl. Sci. NS-45 (1998) 467.
[8] A.G. Petrosyan, C. Pedrini, Preparation of single phase $LuAlO_3$–Ce scintillator crystals, in: P. Dorenbos, C.W.E. van Eijk (Eds.), Proceedings of the International Conference on Inorganic Scintillators and their Applications SCINT95, Delft University Press, The Netherlands, 1996, pp. 498–501.
[9] J.A. Mares, M. Nikl, J. Chval, I. Dafinei, P. Lecoq, J. Kvapil, Chem. Phys. Lett. 241 (1995) 311.
[10] A. Lempicki, C. Brecher, D. Wisniewski, E. Zych, A.J. Wojtowicz, IEEE Trans. Nucl. Sci. NS-43 (1996) 1316.
[11] H. Ishibashi, K. Kurashige, Y. Kurata, K. Susa, M. Kobayashi, M. Tanaka, K. Hara, M. Ishii, IEEE Trans. Nucl. Sci. NS-45 (1998) 518.
[12] C.L. Melcher, J.S. Schweitzer, C.A. Peterson, R.A. Manente, H. Suzuki, Crystal growth and scintillation properties of rare earth oxyorthosilicates, in: P. Dorenbos, C.W.E. van Eijk (Eds.), Proceedings of the International Conference on Inorganic Scintillators and their Applications SCINT95, Delft University Press, The Netherlands, 1996, pp. 309–315.
[13] J.A. Mares, M. Nikl, Acta Phys. Pol. 90 (1996) 45.
[14] R. Diehl, J. Brand, Mater Res. Bull. 10 (1975) 85.
[15] K. Meijvogel, A.J.J. Bos, P. Dorenbos, C.W.E. van Eijk, On the relation between prompt luminescence and thermo-luminescence (TL) properties of some materials, in: P. Dorenbos, C.W.E. van Eijk (Eds.), Proceedings of the International Conference on Inorganic Scintillators and their Applications SCINT95, Delft University Press, The Netherlands, 1996, pp. 159–161.
[16] E.G. Gumanskaya, O.A. Egorycheva, M.V. Korzhik, S.A. Smirnova, V.B. Pavlenko, A.A. Fedorov, Opt. Spektrosc. (USSR) 72 (1992) 215.
[17] A.J. Wojtowicz, J. Glodo, A. Lempicki, C. Brecher, Condens. Matter 10 (1998) 8401.
[18] J.A. Mares, M. Nikl, J. Chval, J. Giba, K. Nejezchleb, D. Clement, J.-F. Loude, C. Morel, Development and characterisation of Czochralski grown $Lu_xRE^{3+}{}_{1-x}AlO_3$:Ce crystals ($RE^{3+} = Y^{3+}$ and Gd^{3+}), Rad. Eff. Def. Sol. 150, Part II (1999) 59.
[19] J.A. Mares, N. Cechova, M. Nikl, J. Kvapil, R. Kratky, J. Pospisil, J. Alloys Compounds 275–277 (1998) 200.
[20] J.A. Mares, M. Nikl, E. Mihokova, J. Kvapil, J. Giba, K. Blazek, J. Lumin. 72–74 (1997) 737.
[21] R. Brun, F. Bruyant, M. Maire, A.C. McPherson, P. Zanarini, GEANT 3, CERN DD/EE/84-1, 1987.
[22] M. Ishii, M. Kobayashi, Prog. Cryst. Growth Charact. Mat. 23 (1992) 245.
[23] A. Lempicki, J. Glodo, Nucl. Instr. and Meth. A 416 (1998) 333.
[24] R.H. Bartram, D.S. Hamilton, L.A. Kappers, A. Lempicki, J. Lumin. 75 (1997) 183.